ANNALS OF GEOPHYSICS, 68, 4, DM444, 2025, doi:10.4401/ag-9292
OPEN ACCESS

Drone-based photogrammetry and morphological characterization of the Salse del Dragone mud volcanoes: integrating multidisciplinary data for future exploration

Arianna Pesci[*,1], Giancarlo Tamburello[1], Giordano Teza[2], Enrico Paolucci[2], Martina Zanetti[2]

(1) Istituto Nazionale di Geofisica e Vulcanologia, Sezione di Bologna, Bologna, Italy
(2) Alma Mater Studiorum University of Bologna, Department of Physics and Astronomy, Bologna, Italy

Article history: received February 17, 2025; accepted June 11, 2025

Abstract

This study investigates the Salse del Dragone mud volcanoes, located in the Apennine region of Italy, using an integrated approach that combines drone-based Structure-from-Motion (SfM) photogrammetry, morphological analysis, and the integration of diverse datasets. The primary focus is on high-resolution terrain mapping and characterization through SfM-derived data. The observations were made using point-to-reference primitive distance thematic maps to emphasize the main features of the distributions of the measured points on the ground. Detailed surface features, including active gas emission points and surrounding topography, are thoroughly analyzed. The research also incorporates additional subsurface data obtained from passive seismic measurements, gas emission records, and satellite imagery to develop a comprehensive understanding of the area's dynamics. These efforts aim to estimate the extruded mass volume and assess the spatial distribution of the phenomenon, which appears to be more extensive than previously thought. The study reveals significant morphological anomalies, highlighting the need for further investigation, which will soon be extended to neighboring areas. This research is part of the PROMUD project, funded by the National Institute of Geophysics and Volcanology (INGV).

Keywords: Mud Volcanoes; Landforms; Structure-from-Motion (SfM); Passive Seismic Measurements; Data Integration

1. Introduction

Mud volcanoes are distinctive geological formations due to upward movement of gases, fluids, and fine materials from deep within the Earth. The emitted material typically consists of methane, saltwater, and clay or other fine-grained sediments, which can be released through a central emission conduit, either singular or with lateral branches. This mixture, largely composed of clay and fragmented rock, flows in response to the terrain's morphology,

similar to lava flows from igneous volcanoes (Mammino, 2014). The morphology of a mud volcano is primarily determined by the properties of the extruded material. Overlapping flows often form a conical structure, with steeper sides as the viscosity of the erupted material increases. In contrast, when the material is water-rich, the cone tends to have a gentler slope, with the flows spreading over wide areas, extending far from the emission point. At the summit of a mud volcano, a caldera-like depression often forms, resulting from either intense eruptions or gradual collapse due to continuous material removal. Mud volcano cones can vary significantly in height and size, from a few centimeters to several hundred meters, while volcanic clusters may span several kilometers (Dimitrov, 2002; Jung and Grasso, 2014).

These phenomena are typically found in areas with compressive tectonics, where tectonic plates converge, but also in basins with high sedimentation rates, such as large river deltas. A critical factor in mud volcano formation is the presence of a source layer composed of thick sequences of fine-grained, poorly consolidated sediments with relatively low density. These sediments trap fluids, which, under the pressure of overlying layers and continuous deposition, become overpressurized. Tectonic forces, dehydration of clay-rich materials, and hydrocarbon formation further increase this pressure. Among the hydrocarbons, methane, being lighter, rises more quickly to the surface and is commonly detected in mud volcano areas (Mazzini et al., 2009).

Mud volcano formation could be understood as a sequence of interconnected events. Gravitational instabilities, driven by fluid overpressure, trigger the fracturing of overlying, more rigid layers, ultimately leading to the surface release of material. Gravitational instability involves clay-rich sediments (shales), having plastic behavior, propagating through denser layers to form dome-like structures. Fluid overpressure is linked to hydrocarbon generation within unstable shales or surrounding sediments. Hydraulic fracturing, facilitated by increased fluid pressure, tectonic stresses, fault reactivation, or seismic activity, allows the pressurized movement of gas, water, and sediments to the surface. Permeable fractures provide a pathway for these materials to migrate upward (Bonini, 2009; Martinelli and Judd, 2004; Etipoe et al., 2007; Mazzini and Etipoe, 2017; Zanetti, 2024).

Mud volcanoes are widespread across the globe, with thousands occurring on land and many more along continental slopes and underwater plains. They are commonly found in clusters across regions such as Europe, Asia, the Americas, and Oceania. A striking example is Azerbaijan, where mud volcanoes feature towering cones, large calderas, and vast areas affected by the phenomenon. Numerous other examples exist worldwide, including tragic events caused by sudden eruptions (Kopf, 2002; Mikov, 2005; Aliyev, 2024).

In Italy, these fascinating formations are primarily found in the clay-rich regions of the northern Apennines and Sicily, where underground gas and fluids interact with soft sediments, creating dynamic and constantly changing landscapes. Notable examples include the Salse di Nirano in Emilia-Romagna and the Maccalube di Aragona in Sicily, where bubbling pools of mud and periodic eruptions provide striking spectacles. These sites, both of which are Italian Nature Reserves, not only provide insight into the geological processes beneath the surface but also represent unique environments of scientific and natural value (Accaino et al., 2009; Lupi et al., 2016; Gattuso et al., 2021; Antunes et al., 2022; Brindisi et al., 2024; Cafagna et al., 2024; Gianbastiani et al., 2024). In order to study mud volcanoes, the INGV multidisciplinary three-year project (2023-2025) called PROMUD (definition of a multidisciplinary monitoring PROtocol for MUD volcanoes) was proposed and is currently being implemented (https://progetti.ingv.it/en/promud). The final goal of PROMUD is to detect precursors and identify the main indicators of the evolution of activity towards paroxysm. The project is based on the integration of the analysis of geophysical (seismic, magnetic, geoelectric, and environmental radioactivity), geodetic (GNSS and tiltmeters), bio-geochemical (characterization of emitted fluids and vegetation analysis), topographic, and geomorphological data acquired primarily from two highly monitored study areas: the Maccalube di Aragona and Salse di Nirano sites. However, other mud volcano areas are also considered within the framework of this project.

The geological context of the northern Apennines is shaped by the closure and subduction of the Ligurian-Piedmont Ocean, marked by thrust tectonics during the orogenic phase. This phase involved compressive forces migrating eastward, while a back-arc extensional trend from the Middle Miocene to the Quaternary led to significant crustal thinning. The Adriatic margin's lithologies were progressively deformed and incorporated into the Apennine chain, which is primarily composed of Mesozoic and Tertiary carbonates (Sanità et al., 2024). The geology of the lower Apennines facilitated mud volcano formation, as evidenced by numerous emissions along the diagonal discontinuity between the Apennines and the plain. Studying these areas requires a multidisciplinary approach, integrating geochemical, seismic, and remote sensing techniques (Marestrelli et al., 2019).

Remote sensing plays a key role in enhancing our understanding of mud volcanoes, especially in the study of their morphology. Techniques like Structure from Motion (SfM) photogrammetry and LiDAR create high-resolution

3D models of the terrain, enabling detailed analysis of mud volcano features (Smith et al., 2016; Giordan et al., 2020; Pesci et al., 2023). These models help identify features such as height, volume, morphological changes over time, and the spatial distribution of volcano emissions. Periodic remote sensing campaigns allow for monitoring the evolution of mud volcanoes, tracking changes in size, shape, and areas impacted by emissions. Surveying carried out with an Unmanned Aerial System (UAS) is an invaluable tool, especially for accessing difficult or hazardous areas, making it ideal for studying active craters or unstable zones prone to landslides (Gessesse et al., 2017; Barbieri, 2020; Zhang et al., 2021). In general, remote sensing techniques could complement traditional methods like geochemical, seismic, and thermal surveys, by combining morphological data with gas emission measurements and providing further insight into the internal processes driving mud volcano activity. This approach can lead to a more comprehensive understanding of mud volcano dynamics, potentially aiding in the assessment of geological risks, such as landslides or eruptions, and supporting the management and preservation of geo-sites with scientific and tourist value. In this context, remote sensing offers valuable perspectives on mud volcano morphology and processes, helping guide scientific research, environmental monitoring, and land management (Tomastik et al., 2019; Fabris et al., 2023).

This article presents the results of a SfM survey carried out in June 2024 at the Salse del Dragone site, located in the municipality of Monterenzio (BO). Using the Structure from Motion (SfM) technique, this innovative methodology enables the creation of detailed 3D models from overlapping images. Data were collected by means of an UAS, offering high-precision aerial views and operational flexibility, even in difficult-to-access areas (enterprise.dji.com/it/matrice-350-rtk).

The primary goal of this campaign was to generate a high-resolution 3D model of the study area, serving various applications, including geomorphological analysis, mudflow monitoring, and tracking temporal changes at the site. The SfM data were also integrated with other datasets, such as gas emission measurements, passive seismic surveys, and historical records of significant past events. This multidisciplinary approach highlights the importance of an integrated methodology for a comprehensive understanding of the Salse del Dragone's complex dynamics, providing new insights for studying and managing these natural phenomena.

2. Geological and morphological overview of the Salse del Dragone area

The Salse del Dragone are mud volcano systems renowned for their intense past activity, now marked by minimal emissions located along the right slope of the Rio Lovinazzo, which gives rise to a landslide. Pyrite samples have been discovered in the area's clays (as reported on the Emilia-Romagna Region website). These mud volcanoes represent the most prominent manifestations of their kind in the province of Bologna. Situated in the valley of the river with the same name, a left tributary of the Sillaro stream, they have formed a clayey plateau. The position and size of these mud volcanoes are in constant flux, and their activity appears to have been far more vigorous in the past, when recurring eruptions earned them the name "Il Dragone" ("The Dragon"). Historical records document the paroxysms of the Salse del Dragone, detailing dramatic phenomena such as the formation of sinkholes, deep rumblings, ground swelling, and the opening of eruptive vents, with expulsions of liquid clay reaching significant heights. Notable events occurred in 1780, and in 1873, massive flows resembling mud torrents were reported, accompanied by gas emissions and flames. These events are described in the 1881 edition of the Guida dell'Appennino, reporting citation by Bombicci (1880, 1882) publications.

The salse emissions are driven by methane gas, oil pockets, and fossil seawater found at depth. These substances ascend due to the internal pressure within the reservoir, softening the clays and producing salty muds of varying densities (hence the term "Salse"). In the case of the Salse del Dragone, the materials involved are primarily scaly clays ("Argille Scagliose"). Small mud volcanoes form at the emission points, reaching different heights depending on the mud's density; highly fluid materials create bubbling craters, while denser muds form mounds that can exceed one meter in height. From the emission area, a large landslide extends downward, reaching the valley floor of the Rio Sassuno (Maestrelli et al., 2019).

Figure 1 presents the geological map of the area, based on data from the Emilia Romagna Region website (technical and geological map), with a new graphical enhancement for a more detailed description of key elements, including geological formations and deposits. The figure is divided into two subfigures to avoid overlap and fully display the relevant features, with dashed lines outlining their boundaries. The map highlights both pre-Quaternary geological units and Quaternary deposits, which cover much of the Apennine region. The Quaternary deposits in the northern

Apennines exhibit significant variability due to diverse depositional environments, climatic changes, and tectonic dynamics that have shaped the region during this period. The study area primarily features fluvial and colluvial deposits, including gravels, sands, alluvial silts, fluvial terraces, and unconsolidated materials (clays, sands, and gravels) resulting from erosion, landslides, and washout processes. The orange circle in the figure indicates the mud volcano zone, where the main eruptive vents are located. The yellow closed line defines the actual study area. As shown by the overlap with the geological map, the study area is slightly smaller than the full extent of the mapped landslide and mud deposits – particularly in the lower portion – because the investigation was limited by natural and anthropogenic boundaries. In fact, the western boundary of the area is marked by an unpaved road separating the slope from cultivated fields, while the eastern boundary is delimited by a dense forest cover. For this reason, the area outlined in yellow represents the portion that can be studied without disturbance and was therefore selected as the effective area of investigation. For further details, please refer to the geological and structural thematic maps available on the Emilia Romagna Region website (ambiente.regione.emilia-romagna.it).

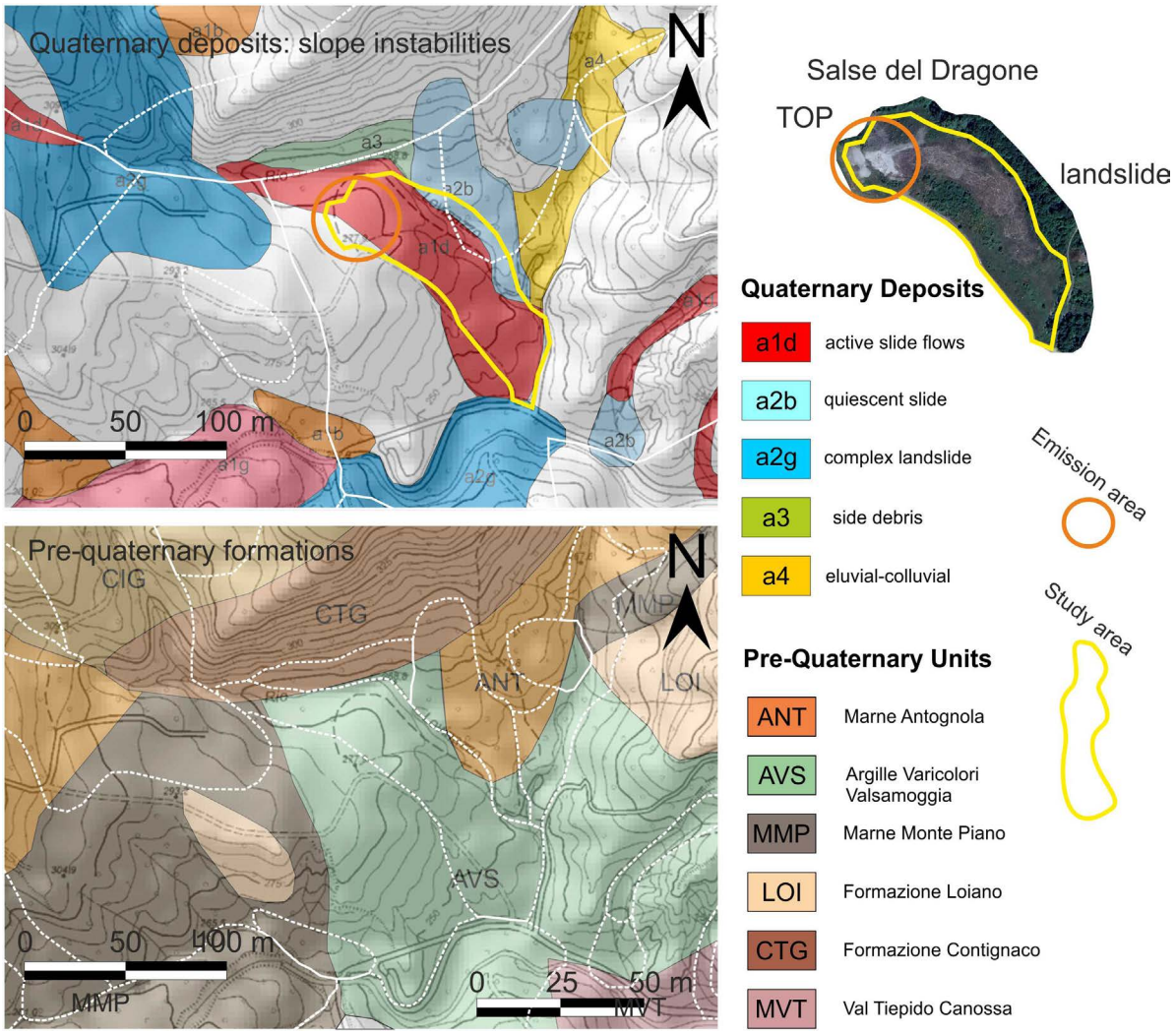

Figure 1. Geological map illustrating two primary categories of information: Quaternary deposits and pre-Quaternary units. To enhance readability, boundaries of the identified units have been superimposed. In the upper part of the figure, an orthophoto of the Salse del Dragone displays the emission zone and the flow path extending downslope, formed by material accumulated over centuries and classified as a landslide deposit. The orange circle highlights the mud volcano emission area, including the main active vents, while the yellow polygon outlines the actual study area. As visible in the overlay with the geological map, the study area is slightly smaller than the full extent of the deposits, mainly due to practical constraints: it is bounded to the west by a dirt road separating it from cultivated fields, and to the east by dense woodland. Therefore, the yellow outline corresponds to the accessible and non-disturbed area suitable for investigation.

The area is located in the lower Apennines, characterized by a varied landscape with hilly and mountainous terrain of moderate elevation, rounded summits, and steep slopes shaped by valleys carved over time by flowing water. Alluvial deposits are predominant, reflecting the dynamic geomorphological evolution of the area. This region is characterized by a series of ridges and depressions, aligned northwest-southeast, following the geological framework of the Northern Apennines. Due to a combination of clayey and sandy soils with low cohesion, steep slopes, and the erosive forces of rainfall, the Bologna Apennines are particularly prone to landslides. These include rotational slides, flows, and surface material movements, often triggered by intense precipitation or anthropogenic activities. The interplay of tectonic processes and climatic factors results in a dynamic landscape, making the area particularly sensitive to geomorphological changes. The regional geomorphology is a product of both long-term geological processes and more recent environmental influences, requiring ongoing monitoring to mitigate geological hazards and ensure land-use sustainability. The dynamic nature of the region, with its pronounced susceptibility to landslides and geomorphological changes, highlights the importance of advanced monitoring techniques. In this context, space-based observations and aerial views become invaluable tools for accurately tracking and understanding the ongoing processes.

The maps provided by the EGMS (European Ground Motion Service) offer high-precision data on ground movements, utilizing InSAR (Interferometric Synthetic Aperture Radar) data provided by Sentinel-1 constellation of the Copernicus program. This service generates detailed surface change overviews through the processing of time-series data, available since 2015. In the specific case of the areas surrounding the Salse del Dragone, the EGMS data reveal the presence of natural scatters, i.e. stable radar reflectors, which allow for accurate monitoring of surface deformations (Costantini et al., 2023; Martins et al., 2024). The analysis shows significant vertical ground variations, with annual subsidence rates in some areas reaching up to approximately 1 cm/y. These findings underscore the ongoing instability of the terrain, which is a typical characteristic of the Apennine region, where debris covers and Quaternary formations contribute to frequent land movements. Moreover, since 2015 the temporal time series of vertical movements are available to characterize the modern perspective of surface dynamics, showing a characterization of ground movements. Unfortunately, in highly vegetated zones, the density of natural permanent scatters is low, and they are sparsely distributed in the area. However, the available ones contribute to more informed land management strategies and the mitigation of natural hazards.

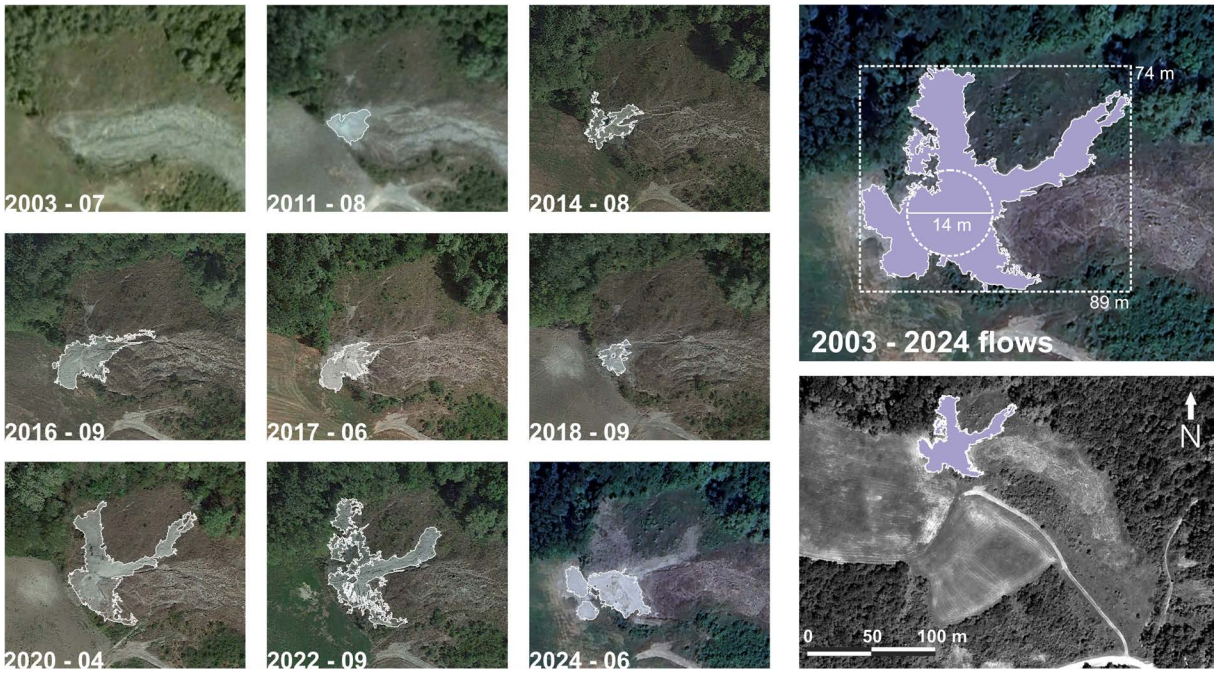

Figure 2. Multitemporal images downloaded from Google Earth, processed to enhance colors and contrast, and to automatically extract the boundaries of flows and emissions. The images span from July 2003 to June 2024, including data from a photogrammetric survey. On the right, a cumulative image displays all flow areas overlaid, with a zoomed-in view providing detailed metric references. The distribution of emitted material is in agreement with the area's topography.

The accessibility of free satellite and aerial imagery has proven to be a crucial tool in land studies and environmental monitoring, offering a wealth of data for various applications. Platforms such as Google Earth stand out for their user-friendly interface and versatility, allowing researchers, planners, and the general public to explore and analyze landscape features with ease. These resources support not only academic research but also the broader dissemination of information, fostering informed decision-making and enhanced land management practices. Furthermore, such tools are invaluable for long-term monitoring and documentation of geophysical changes, contributing to better preparedness for potential natural hazards (Berthaz, 2015).

As previously mentioned, the present activity of the Salse del Dragone is characterized by low-intensity phenomena, with no significant paroxysms or explosive events. Instead, sporadic emissions occur, accompanied by flows of mud that gradually slide down the slope, following the natural contours of the terrain. While these processes are less dramatic compared to historical eruptions, they still reflect the ongoing, albeit subdued, geological dynamics of the area. Figure 2 illustrates the activity from 2003 to 2024, highlighting detected flows. Image optimization techniques available in CorelDRAW (https://www.coreldraw.com) were used to enhance contrast and clarity, making features more distinguishable. Additionally, the Quick Trace function was applied to efficiently extract contours, converting raster data into vector outlines for a clearer representation of flow patterns over time.

Unless there are sources, publications, or studies that could not be accessed, it is noted that this area was never thoroughly studied. Therefore, this chapter aims to provide a foundational understanding on which further research can be built. The following sections present a detailed description of the SfM survey and an analysis aimed at uncovering new insights.

3. Photogrammetric Survey of the Salse del Dragone area

As above mentioned, SfM is widely used in geological and geomorphological surveying due to its efficiency in generating detailed, photorealistic point clouds and digital models from image sequences. These images are typically captured using either ground-based or aerial platforms, often UASs, or a combination of both. The role of SfM is particularly valuable in challenging environments, such as the Salse del Dragone mud volcanoes, where high-precision data is required to analyze complex topographies. In high-precision surveying, especially in geologically complex regions like this site, selecting the right equipment is crucial for ensuring accurate results. Using full-frame cameras, rather than compact ones, is the key to avoiding calibration issues and maintaining geometric stability. Full-frame cameras are less prone to optical distortions, offer better focal length accuracy, and are less affected by thermal and mechanical variations. These advantages make full-frame cameras, obviously coupled with lenses of equal quality, ideal for high-resolution photogrammetry, as they help reduce errors such as the rolling shutter effect, ensuring reliable calibration and high-quality data collection (Westoby et al., 2012; Pesci et al., 2020; Pesci et al., 2022). The photogrammetric survey of the Salse del Dragone took place in June 2024 using a Matrice 350 drone equipped with a ZenMuse P1 full-frame camera. This camera, specifically designed for aerial surveys, features a 35 mm focal length, ensuring the high geometric accuracy necessary for detailed photogrammetric analysis and precise landscape imaging (Stroner et al., 2021). The drone flew at an altitude of approximately 110 m, capturing 167 images along a carefully planned flight path. This path was designed to ensure a 70% overlap between consecutive images, both longitudinally and transversely. The total surveyed area covered approximately 0.1 km^2, roughly double the size of the zone impacted by the mud volcanoes and the landslide. Detailed information about the camera, drone, survey parameters, and data processing methods using Metashape software (www.agisoft.com) is provided in Table 1, which was crucial for the final analysis of the photogrammetric data.

The flight path was continuously corrected in real-time using a precise Real-time kinematic positioning (RTK) applied to data provide by a GNSS receiver, ensuring accurate georeferencing throughout the survey. Spatial positioning corrections were transmitted via Wi-Fi and mobile network, achieving horizontal accuracy of less than 2 cm and vertical accuracy of less than 3 cm. These corrections greatly improved the precision of the data acquisition, enabling detailed analysis of the terrain's surface deformations. The image coverage and the overlap are shown in Fig. 3b of the following chapter, alongside the preliminary product of the SfM analysis.

Table 1. Summary of data related to acquisition and processing. The Surveying section (left column) outlines the main data concerning the camera and drone, while the Photogrammetric Processing section (right column) provides details on SfM data processing and 3D model generation. In addition to the dense point cloud, Metashape produces the triangulated model (triangular mesh), the Digital Elevation Model, and the orthomosaic image. The ground sampling distance (GSD) refers to the mean flying altitude. For further information about instruments and data processing, please refer to the official websites of DJI and Agisoft.

Surveying		Photogrammetric processing	
Camera	DJI Zenmuse P1	Tie points	138 k
Focal length	35 mm	Cameras	167
Aperture	f/2.8-f/16	Aligned cameras	167
Sensor size	8192 × 5460 px^2	Coordinate System	WGS84
Sensor size	35.9 × 24 mm^2	Point cloud points	138180
UAV	Matrice 350 RTK	RMS reprojection error	0.16 px
Weight	6.47 kg	MAX reprojection error	0.47 px
Battery	TB65	Camera location errors	5.2 cm
Max speed (m/s)	23 m/s (~80 km/h)	Dense point cloud	63.12 M
Max Flight time	55 min	Point colors	3 channel (RGB)
Navigation Systems	GNSS	Model faces	5.71 M
RTK accuracy horizontal	1 cm + 1 ppm	Vertices	2.86 M
RTK accuracy vertical	1.5 cm + 1 ppm	Texture size	4096
Images number	167	DEM size	11499 × 8807 px^2
Flying altitude	114 m	Model resolution	14.9 cm/px
GSD	1.35 cm/px	Point density	45 points/m^2
Coverage Area	0.113 km^2	Orthomosaic image size	35745 × 24909 px^2

4. Morphological Analysis and Complementary Data

In this chapter, the results of the analyses and management of point clouds are presented to derive maps that are easy and immediately interpretable. It is important to specify that the focus is on morphology, understood in its general meaning as the study of forms. Therefore, the aim is to observe the models obtained from various perspectives to highlight the characteristics of the shapes and the arrangement of the elements of the remotely sensed terrain

4.1 Morphological analysis

The morphology of an area, i.e. its shape and structure, is fundamental to understanding geological processes such as landslides and mud volcanoes. The dynamics of mass movements, like material flow and soil instability, which is crucial for landslide occurrence, can be obtained by studying morphology. For mud volcanoes, morphological analysis is useful to map emission distributions and monitor temporal changes, providing insights into eruption behavior. The 3D models offer precise observations of topographic variations, crucial for predicting and mitigating high-risk natural events.

Until now, the Salse del Dragone area has never been extensively studied through remote sensing to characterize its morphology in detail. Geological maps of Emilia-Romagna highlight a significant landslide originating from the mud emission zone, extending down to the valley floor of the Rio Sassuno. This landslide formed a clayey plain marked by landslide deposits and unstable slopes, which are crucial for understanding ongoing geological processes, monitoring associated risks, and analyzing the events that have shaped the current landscape. A recent study by Paolucci et al. (2025), based on the remote sensing data described here, suggests that the area is currently in a stable condition.

The morphological analysis method, as detailed in Pesci et al. (2012 and 2013) and Teza et al. (2013, 2015, and 2016), is based on creating reference primitives that are used to assess the collected data, specifically the SfM-based point clouds. These point clouds consist of dense datasets where each point is defined by its coordinates and associated RGB color value, derived from images taken by a drone-mounted camera. The method generates maps by calculating the point-to-plane distance, with the reference primitive being a plane, which determines the interpretation of the resulting map. Most of the analysis was conducted using InnovMetric PolyWorks software, a widely recognized tool for advanced point cloud processing, inspection, geometric modeling, alignment, and data visualization. The software also features an intuitive graphical interface that facilitates efficient management of point cloud data. In particular, this tool was employed for 3D data processing, extraction of geometric primitives, and the generation of cross-sections and morphological maps. In the creation of maps, the choice of primitives is essential for interpreting the morphology or geometry of the terrain. While the selection of these primitives can be arbitrary, when chosen purposefully, they allow for more meaningful and insightful results. The key idea is that to properly observe the distribution of terrain features, it's crucial to look from the right perspective. For instance, when the primitive is a plane that interpolates points distributed along a sloping surface, the resulting point-to-plane distance map will highlight the terrain's distribution along that direction, offering a clearer understanding of the morphology. This approach helps emphasize specific geometric features and spatial distributions that might otherwise be less apparent. This approach was applied to the entire surveyed area, also considering the adjacent agricultural zones (Area 2 and Area 3) near the investigated one (Area 1). Here, two prominent areas with positive values (point to plane distance) were identified, indicating localized reliefs and protrusions reaching several meters above. Since there is very little information available on the Salse del Dragone, it seems important to extend the observations to the neighboring areas, which could be an integral part of the mud volcano system, despite the lack of surface evidence at present.

Figure 3 shows some preliminary results of morphological analysis across the entire surveyed area, covering the emission zone, the underlying landslide, and adjacent agricultural surfaces. Despite human modifications, the absence of dense vegetation allows clear observation of the landforms. This preliminary analysis shows a fan-shaped slope distribution with an elevation variation of ~60 m over 300 m (20 m to 100 m inclination). The central part of the model clearly shows the mud volcano surface, and further refinement with point-to-plane comparison offers finer details, enhancing the definition of terrain contours. Despite this marked difference in altitude, the central part of the model (box c) clearly highlights the mud volcano surface, where the mud emissions are distinctly identifiable. This becomes even more evident in the maps in box (d), which are independent morphological maps generated by comparing the points with a reference plane that better represents the specific area, minimizing the deviation from all the points in Areas 1, 2, and 3. The use of point-to-plane calculation, while often subtle, offers added value by isolating vertical variations in the terrain, which is crucial in environments with complex topography or vegetation. In this case, the reference plane was carefully fitted to each area, allowing for a more accurate representation of local morphological features, including those that could be influenced by vegetation. Although it is true that some of the higher sectors in Fig. 5d may reflect the presence of vegetation, the analysis focuses on distinguishing terrain features that are not significantly affected by such cover. The application of point-to-plane differences, much smaller than those observed in the horizontal map (for example, ranging from –6 m to 6 m instead of 0 m to 60 m),

allows for finer nuances in the color distribution, significantly enhancing the definition of terrain contours and making the underlying topographic structure more apparent.

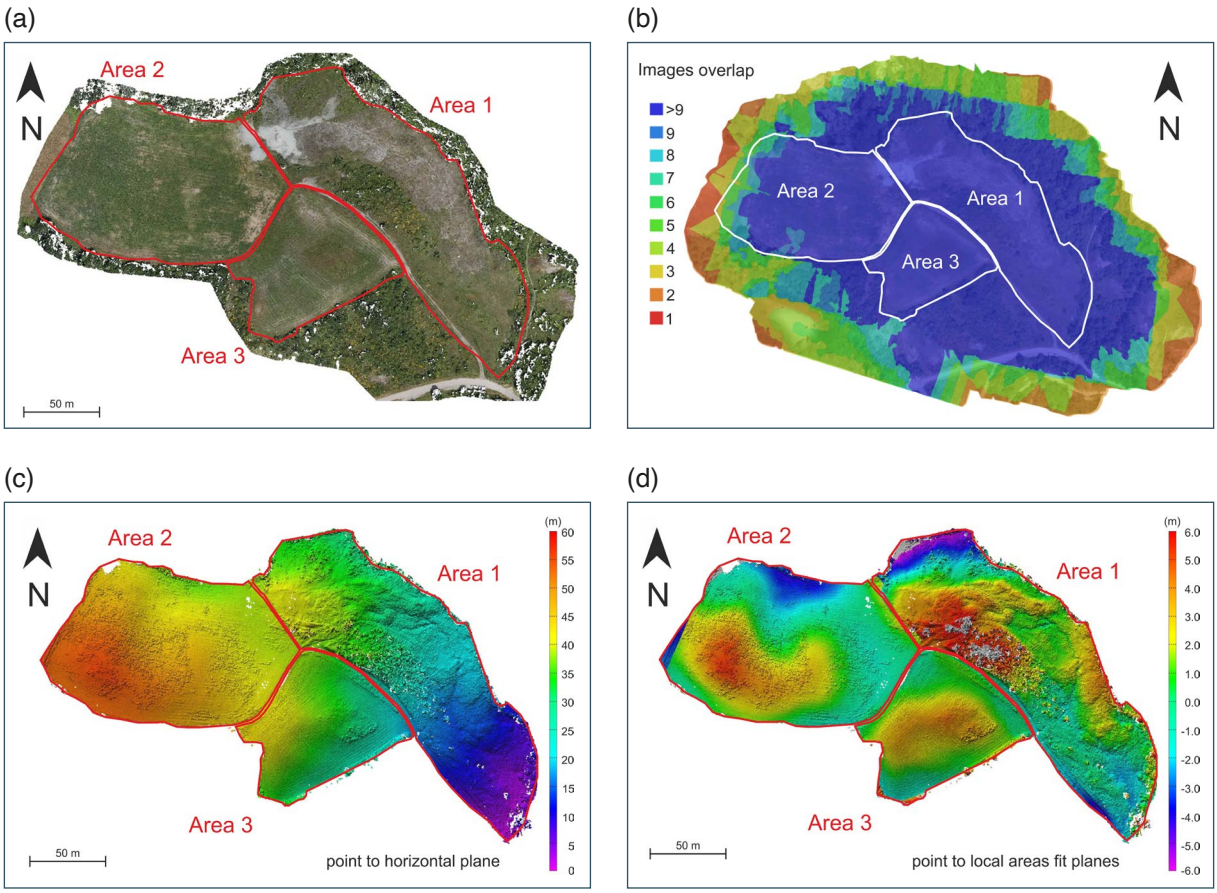

Figure 3. Point cloud representing the entire surveyed area, divided into three sections: Area 1 includes the mud volcano zone, the emission area, and the descending landslide body; Areas 2 and 3 correspond to two cultivated fields. These three areas together form the complete SfM model: (a) Point cloud displayed with natural (photorealistic) colors; (b) the image overlapping for surveying coverage quality; (c) Altimetric map showing the reference horizontal plane, used for the point-to-plane distance calculation, passing through the lowest point of the point cloud; (d) Three independent morphological maps, one for each of the three areas.

4.2 Some satellite image-based observation

While the study focuses on the mud volcano zone and its deposits, adjacent areas may have been involved in similar processes in the past. Using satellite images from Google Earth's multitemporal database, terrain variations were compared, highlighting changes in color, sparse vegetation, and other irregularities. These images, with resolutions up to 30 cm, helped identify subtle anomalies that could indicate past or ongoing geological activity.

Following the procedure described in the previous Figure 2 (contouring mud flows), a visual inspection was performed on other regions exhibiting morphological anomalies, using satellite images from the multitemporal Google Earth database. This approach allowed for the comparison of images from the same area taken in different years, revealing variations in terrain, such as changes in color, areas with sparse or altered vegetation, and other irregularities. When direct evidence of emission phenomena (such as craters, mud volcanoes, springs, or other surface features) is lacking, visual observation becomes crucial. It enables the assessment of chromatic features, with images being enhanced through adjustments to contrast, saturation, brightness, and color tones. This technique highlights subtle details and features that may not be immediately visible, improving the clarity of morphological characteristics and supporting the extraction of additional information for a more comprehensive analysis. Since the

satellite images extracted from Google Earth have a maximum spatial resolution of 30 cm (with older images often having lower resolution), it would be beneficial to have access to a database of higher-quality images to observe land surface irregularities or anomalies with greater accuracy.

Figure 4 shows two satellite images related to Area 3 where some patterns, which seem not due to anthropic management, can be easily detected. The presence of such features suggests that gas emissions from the subsurface may have occurred. This is because such a phenomenon can often induce anomalies in the terrain detectable in satellite or aerial imagery, such as scorched patches of grass or other irregularities in vegetation. These results stem from the interaction between emitted gases and the surface, often showing as patches of withered or dead vegetation, soil color changes, or exposed ground with no apparent natural cause. Subsurface gases like methane and carbon dioxide can damage or kill plants, altering the soil's chemical properties. These visible signs are key for identifying areas where geochemical measurements would be most useful, providing a basis for further investigation.

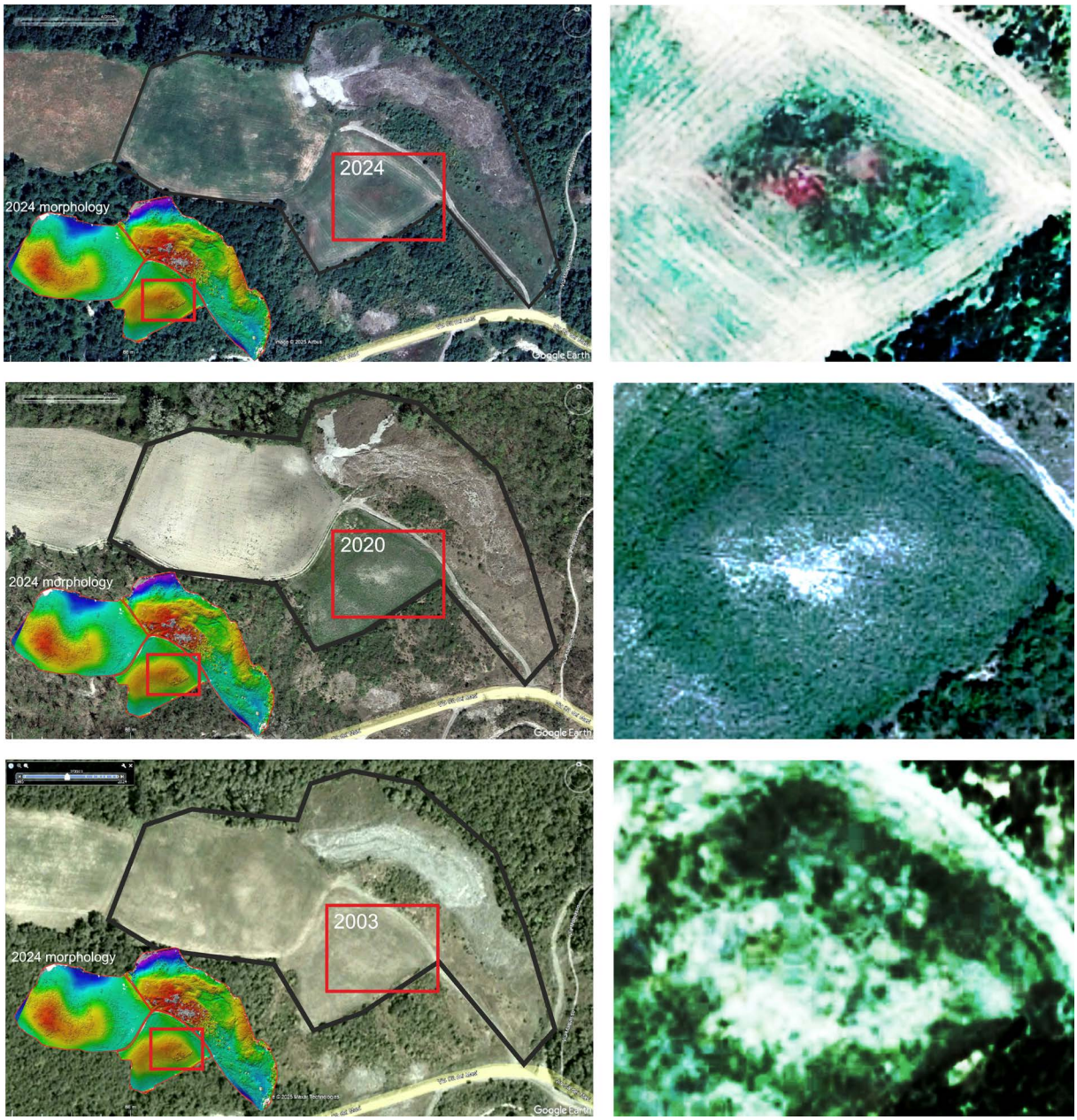

Figure 4. Three images from Google Earth showing a zoomed-in view of Area 3, where the morphology reveals anomalous positive features. Despite the relatively low resolution, a noticeable discontinuity in vegetation is consistently observed across the years 2024, 2020 and 2003. As the area is used for agriculture, anthropogenic activities often disrupt the land, complicating direct comparisons between the images.

Specifically, in Areas 2 and 3, monitoring campaigns focused on methane (CH_4) and carbon dioxide (CO_2) should be carried out using a grid with several-meter sides. This would help detect potential emissions and assess the full extent of the mud volcano area along the studied slope. Some authors use a methodology that combines geophysical and geochemical observations to identify areas where there may be subsurface gas leaks, using the analysis of ground deformations and changes in vegetation patterns that may result from such emissions. Subsurface gas emissions, such as methane or carbon, can affect both the soil and the vegetation above, causing alterations that can be detected through environmental monitoring techniques such as remote sensing and airborne or satellite sensors (Smith and Brown, 2018).

4.3 Features from point cloud inspection by virtual navigation

The photogrammetric point cloud was also used for virtual navigation within the model, enabling an immersive exploration of the different regions of the landslide in Area 1, simulating a walk through the terrain. This approach allowed for a comprehensive view of the photorealistic model, unbound by the limitations of physical observation, with the only constraints being the centimeter-scale resolution and the boundaries of the surveyed area. Figure 5 presents several perspectives of the model captured during navigation, with key morphological features accentuated by dashed lines. Notably, the emission zones, recent mud flows, lava flows, past debris accumulations, and areas with significant vegetation, which are crucial for the morphological analysis of the terrain, are all highlighted. Area 1 is framed by a dirt path on one side and a dense forest on the other. At the highest point lies the emission zone, while moving downward reveals noteworthy accumulations and reliefs. It is important to emphasize that the area remains free from cultivation or other human activities, with vegetation distribution largely determined by soil

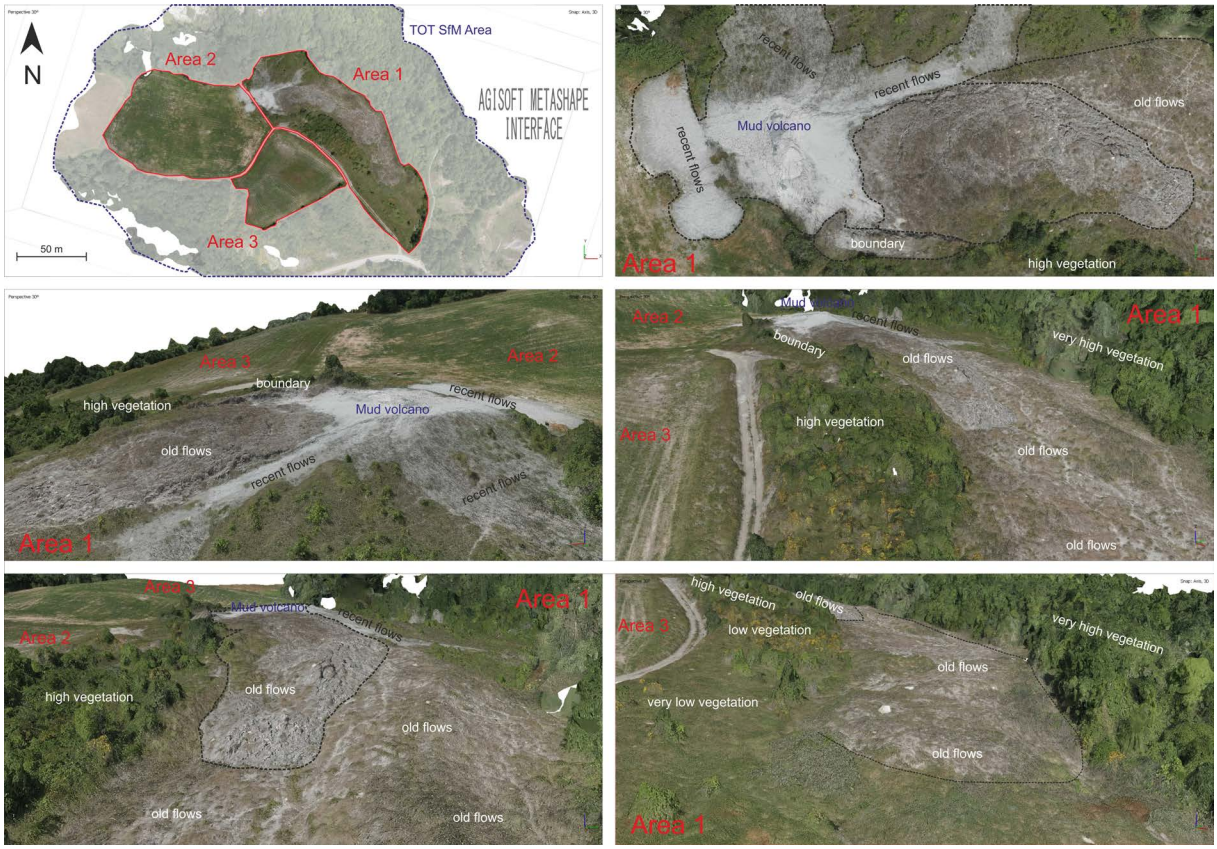

Figure 5. Visual inspection of the SfM point cloud. The views clearly highlight the emission areas, recent flows and their distribution, as well as past flows and accumulations. Additionally, various levels of vegetation present in the area are visible. On the left, a zoomed-in view of the emission area from the orthophoto: red arrows indicate the emission points, while the red circle highlights the operators at work measuring gas.

characteristics. The sparse vegetation in the area, except near the path, is likely linked to the presence of landslide material and the chemical properties of the soil. This observation, along with the previously discussed elements, will inform the planning of future geochemical surveys. Additionally, on the left side of the figure, a detailed view of the plateau's emission area is provided. This section, extracted from the generated orthophoto, offers a thorough analysis of the images acquired during the June 2024 survey. The vents are distinctly identifiable, and the high-resolution imagery enables an accurate representation of the surface features, capturing both the active emission points and the surrounding topography, as well as any morphological changes over time.

4.4 Refined Maps

An additional morphological analysis was carried out specifically on Area 1, i.e. the current Salse del Dragone, where a detailed point-primitives comparison was applied. Three reference planes were used for this analysis: the horizontal plane passing through the lowest point of the landslide, the fit plane representing the overall landslide area, and the fit plane obtained excluding the higher relief and accumulation zones at the top of the selection, such as the emission plateau and the significant accumulation below it.

The results of this analysis, shown in Fig. 6, provide a clearer and more detailed view of the morphological features of the area. Compared to the previous, broader analysis, the elevation map for this smaller, focused area is more readable, revealing greater detail in zones with significant material accumulation. The two fit maps, while displaying subtle variations in spatial distribution and more prominent differences in value magnitudes, offer an excellent means of observing the landslide's structure and the movement of material from the upper to the lower parts of the

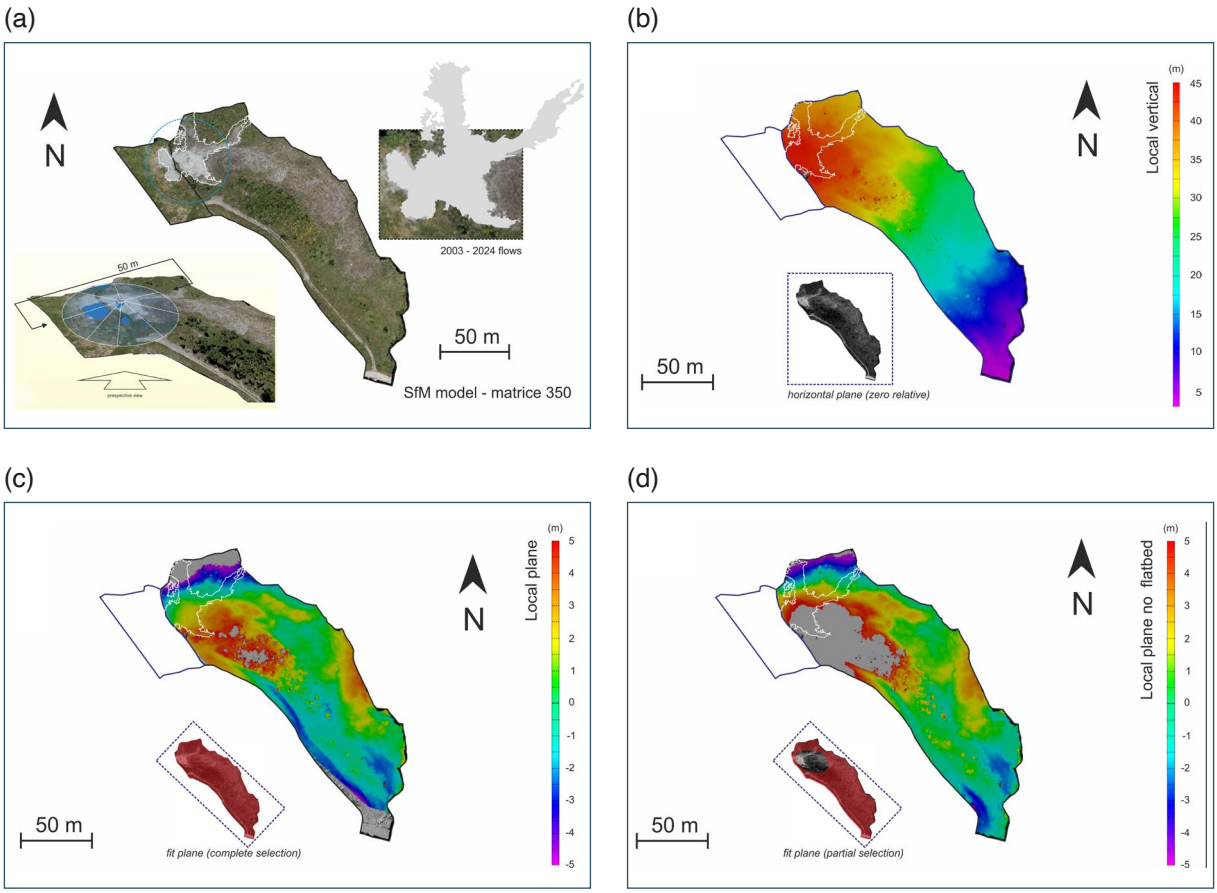

Figure 6. Refined morphological analysis of Area 1: (a) Point cloud highlighting the area of recent flows and emitted material, with the cone defining the bodies of the plateau; (b) Map of the relative elevation of the points; (c) Morphological map based on the fit plane obtained by interpolating all the points (see red selection); (d) Modified morphological map, excluding points from the higher reliefs (see red selection).

slope. The morphological maps, combined with the insights gained from navigation, show that the area housing the emission vents is situated on a plateau, i.e. a slight rise a few meters higher than the surrounding terrain, with steep sides and a relatively flat surface. To further characterize this feature, points from these lateral bands were selected and used to fit a cone-shaped primitive, as shown in panel (a) of Fig. 8, with a base diameter of 50 m.

The maps presented in the figure were chosen for their clarity and comprehensiveness, though it is important to note that many other maps were also produced, ranging from global ones to those focusing on specific sub-areas. The point cloud itself represents the reality, which could be criticized in terms of scale. The use of the RTK system with real-time corrections via mobile network and wireless connection limits the accuracy of position determination to just a few centimeters. The methods used to extract the maps are, in essence, tools for observing the reality, each carrying a degree of inherent subjectivity. For example, while the horizontal plane facilitates the examination of altimetry and the fit plane allows for the analysis of internal distributions relative to a common setup, other approaches, such as an interpolated plane focused solely on peripheral areas, also have their merits. Therefore, the analyses presented in this study are more numerous and detailed than those shown in Fig. 8, although the latter focuses on the most consistent and comprehensive information.

4.5 Volume Estimation through Adapting Passive-Seismic Data

Thanks to portable and versatile instruments such as Tromino or Lennartz LE-3Dlite, seismic noise measurements can now be easily conducted to investigate the subsurface. These instruments measure ground oscillations caused by seismic waves, therefore allowing the analysis of their frequencies and propagation through various layers. In this way, the calculation of layer thicknesses and the identification of their composition can be obtained, providing a non-invasive image of the subsurface. However, the accuracy of layer thickness estimation may be affected by subsurface complexities, such as variations in material density and stiffness, or the presence of thin layers that could fall below the instrument's resolution. Additionally, external noise, such as environmental disturbances, can degrade the signal quality and reduce the reliability of the analysis. These instruments are particularly useful for HVSR (Horizontal to Vertical Spectral Ratio) studies, which assess the spectral ratio between horizontal and vertical seismic components to estimate the resonance frequencies of the ground and evaluate the thickness and stratigraphy of the subsurface (Picozzi et al., 2005; Lunedei and Albarello, 2010; Molnar et al., 2022; Paolucci, 2025).

In 2024, a seismic measurement campaign was conducted at the Salse del Dragone, following similar approaches previously applied at Le Salse di Nirano in the province of Modena. This site has been extensively studied by various institutions and universities. The campaign was carried out by the Department of Physics and Astronomy (DIFA) at the University of Bologna. Both single and aligned measurements were taken using the Tromino instrument, with approximately 30-minute sessions at each point of interest, both on the plateau and within the landslide body. These results, currently being published, are partially presented by Paolucci et al. (2024) and Zanetti et al. (2024), who used geophysical data to assess the slope's stability.

Thanks to the GNSS and RTK positioning system integrated into the Matrice 350 drone, the precise location of each seismic station measurement could be mapped onto the photogrammetric model with centimeter-level accuracy. This enabled the direct correlation of HVSR outputs, subsurface layer depths, and seismic wave velocities with specific areas within the SfM point cloud. Moreover, the availability of a DEM obtained from remote sensing surveys allows for accurate modeling of layer thicknesses based on resonance frequencies, taking into account the dependency of HVSR results on local topography. A detailed discussion of seismic analyses, measurement errors, and interpretation uncertainties is not included here, as these topics are extensively covered in the referenced literature. However, the main result, shown in Fig. 7, is presented here. It consists of scattered data points within the point cloud, used to define thematic areas representing layer depths. While the data are clear and comprehensive, it is important to note the stations located in the upper part of the area, covering part of the plateau and the left-side region, extending a few meters beyond the surveyed area where the emission vents are located. These stations, predominantly represented by blue and light blue dots, indicate significant layer depths and low seismic wave velocities, suggesting the presence of a substantial amount of material, likely of a muddy nature (Zanetti et al., 2024; Paolucci et al., 2024).

The ability to map the depth of subsurface discontinuities in a confined area, yet surveyed with exceptional detail and precision, offers a valuable insight into the structural and geological characteristics of the site. By hypothesizing the division of the area into distinct zones with varying layer depths, the data collected becomes even more robust, paving the way for the creation of a preliminary model of the landslide's underlying bed. This integrated approach

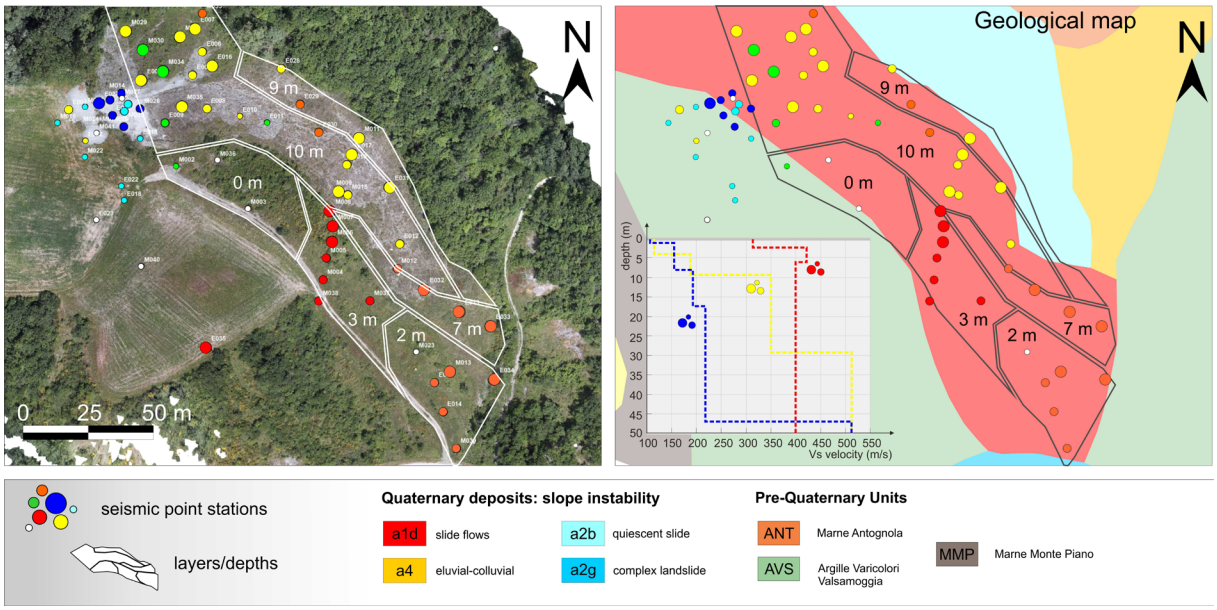

Figure 7. The point cloud and the geological map provide the background for displaying the passive seismic measurement stations. The polylines indicate the division of the area based on average depth estimates of the surface layer. The inset shows an example of HVSR analysis, with seismic wave velocity profiles for different soil materials at various depths. Points within the circle suggest high depth. Locations of the single-station measurements are classified according to resonance frequency and detected peaks, as identified by the corresponding HVSR spectra. The white lines on the map represent the zonation, which was performed based on the spatial distribution of F0 and A0 values. Insets display example HVSR curves for several zones. More details are in Paolucci et al. (2025).

not only enhances the accuracy of the material distribution analysis but also provides a clearer understanding of the landslide's composition. It is suggested that the materials currently constituting the landslide result from both gradual emissions over time and more rapid, episodic events, both of which have shaped and reshaped the landslide body. The passive seismic data, particularly regarding depth, was instrumental in refining the point cloud, allowing for adjustments to be made in the areas shown in Fig. 9. These adjustments involved cropping specific sections and lowering them based on the estimated values. This process led to the reconstruction of Area 1, assuming an initial hypothesis, or "time zero", before any mud material had been deposited, flowed, or emitted on the slope. Consequently, the modified point cloud represents an early state of the site, as though surveyed at an indeterminate time in the distant past, reflecting the underlying processes tied to the formation of mud volcanoes. In order to better understand the internal distribution of materials and to propose a preliminary reconstruction of the landslide evolution, the area was manually subdivided into thematic zones based on the results of the passive seismic campaign. Although the seismic stations were not densely distributed, their spectral responses (HVSR curves) showed recognizable differences in resonance frequency and inferred depth of soft layers. By grouping stations with similar seismic responses, it was possible to delineate areas with presumably homogeneous subsurface characteristics. This subdivision, while not derived from automated clustering or geostatistical interpolation, was done through visual inspection and guided by both geophysical data and morphological cues observed in the photogrammetric model. The resulting separation is therefore partly arbitrary, yet provides a first, pragmatic framework for interpreting the subsurface structure. This integrated approach supports the hypothesis presented in Fig. 8, which illustrates a reconstructed surface corresponding to the hypothesized "time zero" before the accumulation and flow of extruded material began.

Figure 8 presents two models: the current one and the initial model, modified based on passive seismic data. The morphological comparison reveals how, following the adjustments, the area appears more uniform, with fewer discontinuities and a smoother color gradient, except for the upper section along the road, where denser vegetation persists. At first glance, this could indicate that the corrections have successfully reconstructed the pre-debris flow landscape. However, it is important to note that this is no more than a preliminary hypothesis, requiring further verification.

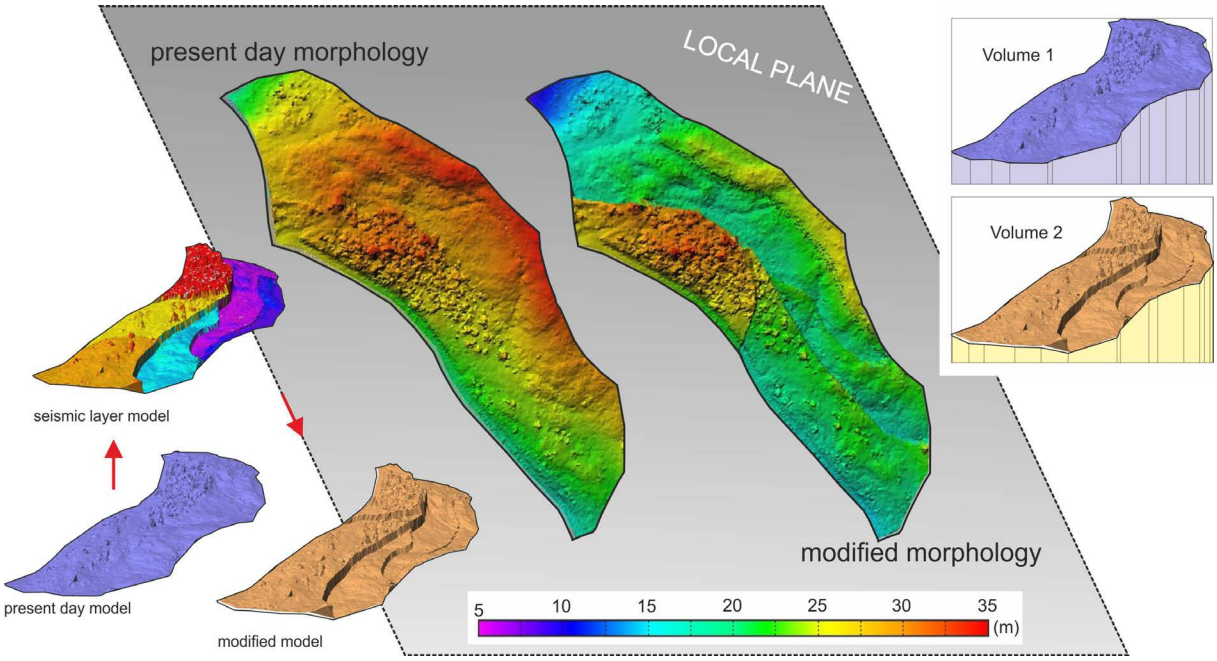

Figure 8. On the left, the model of the area and the mod ified model based on the five zones defined earlier, characterized by discontinuities obtained through passive seismic, are shown. In the center, the morphology of the initial model and the modified one, with respect to a fitting plane obtained by selecting and interpolating the peripheral bands of the area. On the right, the schematic for calculating the accumulated volume from the past to the present.

The procedure for calculating the accumulated volume is thoroughly outlined in Pesci et al. (2018), where the authors developed and compared multi-temporal remote sensing models to estimate the volume of material extruded during a full-scale liquefaction experiment, incorporating both the accumulation of sands and clays and the subsidence effects at the site. In essence, the process involves these stages: co-registration of all the models into a common reference frame; generation of a reference triangulated model, i.e. a triangular mesh where complex geometries are subdivided into small triangular faces; and volume calculation for each model. The difference between these volumes is then computed to obtain the residual of interest. To minimize errors and avoid potential systematic biases, it is critical to maintain a consistent reference plane, ensuring that every element of the model is represented in the same way, thus preserving volume consistency. The difference in volumes between the original model and the modified one, calculated based on the constitutive triangular elements forming 3D elements on the reference plane, is 70.8×10^3 m^3. The error estimate depends on factors such as surface type, triangle size, and the number of elements in the triangulated model. The first factor addresses surface irregularities, particularly in areas with dense vegetation, while the second influences the model's sensitivity to accuracy. As in Pesci et al. (2024), a nearby, nearly independent area (about 1000 m^2) was used to estimate a realistic error value by creating models with varying internal sizes, increasing the average triangle side from 0.2 m to 2 m, and calculating volumes relative to the reference plane. The volume differences resulted in an error of approximately 0.5 to 0.7 m^3 per unit area. For this reason, a relative error of 10% was applied to the volume difference in our previous computation leading to $70.8 \times 10^3 \pm 7.1 \times 10^3$ m^3.

5. Discussion and conclusion

The results achieved so far using different techniques, from remote sensing to geophysical surveys, are here interpreted and discussed in an integrated way, also and above all in order to emphasize the role of multidisciplinarity in the study of a complex system such as a field of mud volcanoes, whose extension is not at the moment entirely certain. Furthermore, some ideas are provided for future measurement campaigns to be implemented in order to investigate the evolution over time of the system as high quality multi-temporal data become available.

The point cloud from the UAS-based SfM survey of the Salse del Dragone marks a key step in the PROMUD project, providing the first high-precision remote sensing data for the area. This detailed model of mud volcano-affected regions in Northern Italy offers geometric, morphometric, radiometric data, and interesting integration with other surveying methods.

Some major findings emerge from an inspection of the point cloud and the morphological maps created through point-to-plane comparisons. The emission area, confined to the upper part of the landslide slope, appears as an elevated plateau with fairly steep sides, resembling the shape of a truncated cone. The plateau surface hosts several emission vents from which gas and liquids escape. Activity, as evidenced by the time series of satellite images, is rather limited, and the flows in the last 20 years have only affected the summit area of the site. The landslide body represents the accumulation of material deposited from distant times, possibly resulting from the documented paroxysms that occurred in 1780 and 1873, or it could be the cumulative effect of these and other past events. Data extracted from passive seismic analysis were used to divide the photogrammetric model into sub-areas, classified on the basis of HVRS results, which provided a reasonable hypothesis about the depth for the surface layer (please see the areas encircled by polylines shown in Fig. 9), and to create a modified model representing the landslide's slip surface (landslide basal surface or landslide bed). The calculation resulted in an estimate of $\sim 70 \times 10^3$ m^3. If this data were to be considered as the total accumulation from the mud volcano system's activity, it seems rather small, possibly even underestimated. Historical records describing a significant eruption (in 1835) at the Montegibbio Mud Volcano in the Modena Apennines, about 60 km away, estimate a paroxysm with an extrusion of 500×10^3 m^3, roughly seven times greater than the calculated value. Part of the seismic station points creates a dispersed cloud relative to the emission plateau, revealing a deep underlying area composed of liquid or muddy material, causing the low velocity of seismic waves passing through this layer. The location of this cluster of stations also closely aligns with the primitive shape of a truncated cone, fitted using points from the lateral surfaces of the emission plateau. This could indicate the presence of a large preferential conduit for the muddy material, suggesting that the mud volcano area might actually have a much larger spatial extent, even though there are currently no direct evidences. This could partly agree with satellite image analyses, which show anomalies in adjacent areas, including alterations in vegetation characteristics that, moreover, coincide in some cases with morphological features highlighted in the overall area's morphological map.

To the best of the authors' knowledge, the mud volcano system considered here, i.e. the Salse del Dragone, has not been studied extensively. The obtained results are therefore original and certainly very interesting for the purpose of a greater understanding of the specific field of mud volcanoes. However, in addition to providing answers to various questions, the study described here has raised other questions, which highlights its limitations and preliminary nature, and therefore underlines the need for further investigation. Therefore, this preliminary work, based on geometric studies, morphology, image observation and processing, and the integration of remote sensing with geophysical measurements, clearly suggests the need to expand the study area to encompass the entire portion of the slope.

The results obtained so far, based on a detailed geometric analysis integrated with passive seismic measurements, guide the planning of the next research steps, which include:

1) SfM surveys regularly carried out monthly or seasonally, to generate highly detailed 3D models and time series of georeferenced, accurate orthophotos for automated processing aimed at detecting anomalies, which may be related to surface alterations caused by chemical processes.
2) A broader, spatially distributed passive seismic survey, focused on specific profiles selected based on preliminary morphological discontinuities, aimed at determining the depth and structure of subsurface layers at greater depths.
3) A geomagnetic survey, designed to measure variations in the local magnetic field, providing insights into buried structures such as potential gas reservoirs or fluid pathways, and helping to verify the hypothesis of relevant natural gas and fluid reservoirs.
4) A geoelectric survey with a sufficiently long distance between measurement points to reach greater depths. This will help us gain a clearer understanding of the subsurface structure beneath the emission zone and provide further insights into the geology of the area.
5) A complete survey across the entire slope area, aimed at detecting methane gas and creating models to integrate with the point cloud, with the goal of identifying potential correlations between surface anomalies and geochemical data.

In conclusion, the integration of various remote sensing and geophysical methods in this preliminary study suggests the potential for much broader spatial and subsurface activity, which will be further explored through the planned extended survey campaigns. These will aim to better characterize and understand the mud volcano system at the Salse del Dragone geo-site. The proposed approach can be applied in any context characterized by similar geophysical processes.

Acknowledgments. The authors wish to acknowledge the valuable support and assistance provided by Paola Cusano, project coordinator of PROMUD. In particular, the used UAS was bought within the PROMUD project (https://progetti.ingv.it/it/promud). Special thanks also go to the colleagues at the National Institute of Geophysics and Volcanology (INGV) and the University of Bologna (UniBo) for their valuable contributions to the organization of missions and constructive discussions on the interpretation and significance of the data.
Thanks to Antonello Piombo and Cristiano Guidi for their field support during the various stages of inspection and survey.

References

Accaino, F., A. Bratus, S. Conti, D. Fontana et al. (2007). Fluid seepage in mud volcanoes of the northern Apennines: An integrated geophysical and geological study, J. Appl. Geophys., 63, 2, 90-101. doi:10.1016/j.jappgeo.2007.06.002.

Aliyev, A. A., I. S. Guliyev and I. S. Belov (2002). Catalogue of recorded eruptions of mud volcanoes of Azerbaijan (for period of years 1810-2001). Nafta-Press, Baku.

Aliyev, A., D. Huseynov, O. R. Abbasov, I. Kangarli et al. (2024). Mud Volcanoes of Azerbaijan: The Unique Natural Objects of the Geoheritage, Geoheritage, 16, 1, 20, doi:10.1007/s12371-024-00931-3.

Antunes, V., T. Planès, A. Obermann, F. Panzera et al. (2022). Insights into the dynamics of the Nirano Mud Volcano through seismic characterization of drumbeat signals and V/H analysis, J. Volcanol. Geotherm. Res., 431, 107619, doi:10.1016/j.jvolgeores.2022.107619.

Barbieri, F. (2020). Monitoraggio di aree alpine inaccessibili con fotogrammetria UAV low cost (Tesi di laurea magistrale), Politecnico di Milano, https://www.politesi.polimi.it/handle/10589/177860.

Béthaz, A. (2015). Studio dell'innesco di frane rapide in un'area campione dell'Appennino Bolognese (Tesi di laurea magistrale). Università di Bologna, Scuola di Scienze, https://amslaurea.unibo.it/id/eprint/8254/1/Bethaz_Alberto_tesi.pdf.

Bombicci, L. (1882). Il sollevamento dell'Appennino bolognese per diretta azione della gravità e delle pressioni laterali. Con appendice sulle origini e sui reiterati trabocchi delle argille scagliose, Bologna: Gamberini e Parmeggiani.

Bombicci, L. (1977). Montagne e vallate del territorio di Bologna. Cenni sulla oro-idrografia, geologia, litologia e mineralogia dell'Appennino bolognese e sue dipendenze, in appendice: Angelo Manzoni, La geologia della provincia di Bologna (Facs. delle ed.: Bologna, 1882; Modena, 1880). Bologna: A. Forni.

Bonini, M. (2009). Mud volcano eruptions and earthquakes in the Northern Apennines and Sicily, Italy, Tectonophys., 474, 3-4, 723-735. doi:10.1016/j.tecto.2009.05.018.

Brindisi, A., N. Carfagna, E. Paolucci, M. Salleolini et al. (2024). The fine structure of seismic emissions from the Nirano mud volcanoes (northern Apennines, Italy): a phenomenological study, Bull. Geophys. Oceanogr., 65, 2, 165-176, doi:10.4430/bgo00437.

Carfagna, N., A. Brindisi, E. Paolucci and D. Albarello (2024). Seismic monitoring of gas emissions at mud volcanoes: The case of Nirano (northern Italy), J. Volcanol. Geotherm. Res., 446, 107993, doi:10.1016/j.jvolgeores.2023.107993.

Costantini, M., F. Brozzetti, B. Delmonte, S. Fiorucci et al. (2023). Validating the European Ground Motion Service: An assessment of vertical ground motion time series. In The International Archives of the Photogrammetry, Remote Sensing and Spatial Information Sciences, XLVIII-4/W7-2023, 247-254. https://isprs-archives.copernicus.org/articles/XLVIII-4-W7-2023/247/2023/isprs-archives-XLVIII-4-W7-2023-247-2023.pdf.

Dimitrov, L. (2002). Mud volcanoes – the most important pathway for degassing deeply buried sediments, Earth-Sci. Rev., 59, 1-4, 49-76, doi:10.1016/S0012-8252(02)00069-7.

Etiope, G., G. Martinelli, A. Caracausi and F. Italiano (2007). Methane seeps and mud volcanoes in Italy: Gas origin, fractionation and emission to the atmosphere, Geophys. Res. Lett., 34, 14, L14307, doi:10.1029/2007GL030341.

Fabris, M., A., A. H. Djamil, M. Monego, A. Pesci et al. (2023). Editorial: Management and monitoring of natural disasters using remote sensing and ground-based data, Front. Earth Sci., 11, 1323627. doi:10.3389/feart.2023.1323627.

Gattuso, A., F. Italiano, G. Capasso, A. D'Alessandro et al. (2021). The mud volcanoes at Santa Barbara and Aragona (Sicily, Italy): a contribution to risk assessment, Nat. Hazards Earth Syst. Sci., 21, 11, 3407-3419, doi:10.5194/nhess-21-3407-2021.

Gessesse, M. D., T. Tadesse and S. Rojstaczer (2017). Exploring Google Earth Engine Platform for Big Data Applications, Front. Earth Sci., 5, 17, doi:10.3389/feart.2017.00017.

Giambastiani, B. M. S., E. Chiapponi, F. Polo, M. Nespoli et al. (2024). Structural control on carbon emissions at the Nirano mud volcanoes – Italy. Mar. Pet. Geol., 163, 106771. doi:10.1016/j.marpetgeo.2024.106771.

Giordan, D., D. Godone and J. Everaerts (2020). The use of unmanned aerial vehicles (UAVs) for engineering geology applications, Bull. Eng. Geol. Environ., 79, 7, 3437-3481, doi:10.1007/s10064-020-01766-2.

Jung, R. A. and M. Grasso (2014). Mud volcano morphology and eruptive characteristics: Evidence from the Southern Apennines, Italy. Geol. Soc. Am. Bull., 126, 7-8, 1035-1050. doi:10.1130/B31087.1.

Kopf, A. J. (2002). Significance of mud volcanism, Rev. Geophys., 40, 2, doi:10.1029/2000RG000093.

Lunedei, E. and D. Albarello (2010). Theoretical HVSR curves from full wavefield modelling of ambient vibrations in a weakly dissipative layered, Earth. Geophys. J. Int., 181, 2, 1093-1108. doi:10.1111/j.1365-246X.2010.04560.x.

Lupi, M., B. S. Ricci, J. Kenkel, T. Ricci et al. (2016). Subsurface fluid distribution and possible seismic precursory signal at the Salse di Nirano mud volcanic field, Italy, Geophys. J. Int., 204, 2, 907-917, doi:10.1093/gji/ggv454.

Maestrelli, D., M. Bonini and F. Sani (2019). Linking structures with the genesis and activity of mud volcanoes: examples from Emilia and Marche (Northern Apennines, Italy), Int. J. Earth Sci., 108, 5, 1683-1703, doi:10.1007/s00531-019-01730-w.

Mammino, P. (2014). I vulcani di fango di Paternò e Belpasso sul versante sud occidentale del Monte Etna (Sicilia) / Mud volcanoes of Paternò and Belpasso on the south western slope of Mount Etna (Sicily Italy). Memorie Descrittive della Carta Geologica d'Italia, 102, 171-182. Retrieved from https://www.isprambiente.gov.it/files2017/pubblicazioni/periodici-tecnici/memorie-descrittive-della-carta-geologica-ditalia/volume-102/memdes_102_mammino3.pdf.

Martinelli, G. and A. Judd (2004). Mud volcanoes of Italy, Geol. J., 39, 1, 49-61, doi:10.1002/gj.943.

Martins, J. E., C. M. Cuenca., B. Davids, G. Zhai et al. (2024). Validation of the European Ground Motion Service with Global Navigation Satellite Systems and Corner Reflectors Over Deforming Areas. In IGARSS 2024 IEEE International Geoscience and Remote Sensing Symposium, Athens, Greece, 2024, 7537-7541, doi:10.1109/IGARSS53475.2024.10641305.

Mazzini, A., A. Nermoen, M. Krotkiewski, Y. Podladchikov et al. (2009). Strike-slip faulting as a trigger mechanism for overpressure release through piercement structures. Implications for the Lusi mud volcano, Indonesia, Mar. Pet. Geol., 26, 9, 1751-1765, doi:10.1016/j.marpetgeo.2009.03.001.

Mazzini, A. and G. Etiope (2017). Mud volcanism: An updated review, Earth-Sci. Rev., 168, 81-112, doi:10.1016/j.earscirev.2017.03.001.

Milkov, A. V. (2000). Worldwide distribution of submarine mud volcanoes and associated gas hydrates, Mar. Geol., 167, 1-2, 29-42, doi:10.1016/S0025-3227(00)00022-0.

Milkov, A. V. (2005). Global distribution of mud volcanoes and their significance in petroleum exploration as a source of methane in the atmosphere and hydrosphere and as a geohazard. In G. Martinelli and B. Panahi (Eds.), Mud Volcanoes, Geodynamics and Seismicity, Springer-Verlag, Berlin/Heidelberg, 29-34, doi:10.1007/1-4020-3204-8_3.

Molnar, S., A. Sirohey, J. Assaf, P. Bard et al. (2022). A review of the microtremor horizontal-to-vertical spectral ratio (MHVSR) method, J. Seismol., 26, 653-685, doi:10.1007/s10950-021-10062-9.

Paolucci, E., E. Lunedei and D. Albarello (2017). Application of the principal component analysis (PCA) to HVSR data aimed at the seismic characterization of earthquake prone areas, Geophys. J. Int., 211, 1, 650-662, doi:10.1093/gji/ggx325.

Paolucci, E., M. Zanetti, M. Antonellini, A. Armigliato et al. (2024). Preliminary characterization of the area of the Salse del Dragone mud volcano (Northern Italy) through surface-wave seismic prospecting, In Proceedings of the GNGTS 2024, Retrieved from https://gngts.ogs.it/atti/GNGTS2024/344/.

Pesci, A., E. Bonali, G. Casula and G. Teza (2012). Metodo basato sulla tecnologia laser scanning per la misura delle deformazioni indotte negli edifici dai sismi o altri eventi distruttivi, in La geofisica al servizio della Protezione

Civile – IX Workshop di Geofisica, Museo Civico di Rovereto, 14 Dicembre 2012, https://www.fondazionemcr.it/UploadDocs/4674_Pesci_Rovereto2012_web.pdf.

Pesci, A., G. Teza, E. Bonali, G. Casula et al. (2013). A laser scanning-based method for fast estimation of seismic-induced building deformations, ISPRS J. Photogramm. Remote Sens., 79, 185-198, doi:10.1016/j.isprsjprs.2013.02.021.

Pesci, A., G. Teza, M. Bisson, F. Muccini et al. (2016). Monitoring of a Coastal Zone by Independent Fast Photogrammetric Surveys: the Case of Monterosso a Mare (Ligurian Sea, Italy), J. Geosci. Geomatics, 4, 4, 73-81, doi:10.12691/jgg-4-4-1.

Pesci, A., S. Amoroso, G. Teza and L. Minarelli (2018). Characterization of soil deformation due to blast-induced liquefaction by UAV-based photogrammetry and terrestrial laser scanning, Int. J. Remote Sens., 39, 22, 8317-8336. doi:10.1080/01431161.2018.1484960.

Pesci, A., G. Teza, V. Kastelic and M. M. C. Carafa (2020). Resolution and precision of fast, long range terrestrial photogrammetric surveying aimed at detecting slope changes, J. Surv. Eng., 146, 4, 04020017-1-13, doi:10.1061/(ASCE)SU.1943-5428.0000328.

Pesci, A., G. Teza, F. Loddo, M. Fabris et al. (2022). Studio di possibili effetti sistematici nelle nuvole di punti SfM da APR: confronti con TLS, distorsioni e metodi di mitigazione, Quad. Geofis., 177, 1-22, doi:10.13127/qdg/177.

Pesci, A., G. Teza and M. Fabris (2023). Editorial of Special Issue: Unconventional Drone-Based Surveying, Drones, 7, 3, 175, doi:10.3390/drones7030175.

Picozzi, M., S. Parolai and D. Albarello (2005). Statistical analysis of noise horizontal-to-vertical spectral ratios (HVSR), Bull. Seismol. Soc. Am., 95, 5, 1779-1786, doi:10.1785/0120040152.

Smith, J. and T. Brown (2018). Detection of gas emissions from the subsurface using terrain anomalies and vegetation changes, J. Environ. Geochem., 45, 2, 123-135, doi:10.1016/j.envgeo.2018.03.002.

Stroner, M., R. Urban, J. Seidl, T. Reindl et al. (2021). Photogrammetry Using UAV-Mounted GNSS RTK: Georeferencing Strategies without GCPs, Remote Sens., 13, 7, 1336, doi:10.3390/rs13071336.

Teza, G. and A. Pesci (2013). Geometric characterization of a cylinder-shaped structure from laser scanner data: development of an analysis tool and its use on a leaning bell tower, J. Cult. Herit., 14, 5, 411-423, doi:10.1016/j.culher.2012.10.015.

Teza, G., A. Pesci and S. Trevisani (2015). Multisensor surveys of tall historical buildings in high seismic hazard areas before and during a seismic sequence, J. Cult. Herit., 16, 3, 255-266, doi:10.1016/j.culher.2014.06.008.

Teza, G., A. Pesci and A. Ninfo (2016). Morphological analysis for architectural applications: comparison between laser scanning and Structure-from-Motion photogrammetry, J. Surv. Eng., 142, 3, doi:10.1061/(ASCE)SU.1943-5428.0000172.

Westoby, M. J., J. Brasington, N. F. Glasser, M. J. Hambrey et al. (2012). Structure-from-Motion photogrammetry: A low-cost, effective tool for geoscience applications, Geomorphology, 179, 300-314, doi:10.1016/j.geomorph.2012.08.021.

Zanetti, M. (2024). Mud volcanoes: Salse del Dragone study case. PhD thesis, Università di Bologna, in Numerical Approaches to Slope Analysis: Stability and Collapse Dynamics.

***CORRESPONDING AUTHOR: Arianna PESCI**,
Istituto Nazionale di Geofisica e Vulcanologia, Bologna, Italy
e-mail: arianna.pesci@ingv.it